International Journal of Engineering and Information Systems (IJEAIS)
ISSN: 2643-640X
Vol. 10 Issue 3 March - 2026, Pages: 15-20

Impurity Detection in Metallic Samples Using Laser-Induced Breakdown Spectroscopy (LIBS)

[1]Mohammedain Adm Alhgabo Belal, [1]Aladein Mohammed Daoud Mohaoud , [1]Aldosogy Omar Hamed , [2]Ali Saleh Ali Saleh [3]Salma Adam Hassan Ali , [4-5]Adam .M.A Bakheet , [6-7]Mona A. Abdalrasool and[7-8]Abdalsakhi.S. Mohammed

[1]University of Kordofan Faculty of Science -Department of Physics
[2]University of Kordofan Faculty of Education -Department of Physics
[3]Nyala University, Faculty of Education, Department of Physics & Nyala Technical College Nyala, Sudan
[4]University of Gezira ,Faculty of Science ,Department of Physics and Astronomy ,Wad Madani ,Sudan
[5]University of Sao Paulo, Faculty of Science , Department of Physics ,Sao Carlos ,Brazil
[5]Department of Material Science, Faculty of Science & Technology, Al-Neelain University, Khartoum, Sudan
[6]Department of Physics, College of Science, Sudan University of Science and Technology - Khartoum- Sudan
[7]Department of Physics Laser and Renewable Energy -Faculty of Science and Technology - Al-Neenlen University – Khartoum- postal code- Sudan
[8]Renewable Energy Center - Neenlen University - Khartoum- Sudan.

Abstract: *Laser-Induced Breakdown Spectroscopy (LIBS) was employed to identify and quantify trace impurities in five metallic samples (gold, aluminum, cobalt, iron, and lead), each weighing 5 g. To enhance detection sensitivity and isolate non-matrix emission lines, the reference spectrum of each pure metal was subtracted from the corresponding sample spectrum. The resulting impurity spectra were analyzed using known atomic transition parameters, and the corresponding element concentrations were determined through calibration curves. The gold sample exhibited moderate levels of O, Hg, S, Ca, and Cl, whereas the aluminum sample showed significant contamination by, Mg, F, Cl, and Si, consistent with alloying processes and surface treatment. The cobalt sample exhibited high purity, with all detected impurities present at concentrations below 0.2 ppm. The iron sample exhibited the highest impurity concentrations, primarily consisting of Si and Mg, confirming its alloyed nature. The lead sample showed low-level contamination by, Ca, In, Zn, and Sn. The results demonstrate that LIBS, combined with reference spectrum subtraction, provides a rapid, sensitive, and reliable approach for impurity detection in metallic materials.*

Keywords: Laser-Induced Breakdown Spectroscopy (LIBS); impurity analysis; metallic samples; reference spectrum subtraction; calibration curves; trace detection; alloy characterization; plasma emission spectroscopy.

1. INTRODUCTION

The detection and quantification of impurities in metallic materials are essential for ensuring product quality, verifying alloy composition, and monitoring contamination during manufacturing and processing. Even trace-level impurities can significantly affect the mechanical, electrical, and chemical properties of metals, underscoring the importance of rapid and accurate analytical techniques highly valuable in both industrial and research environments.

Laser-Induced Breakdown Spectroscopy (LIBS) has emerged as a powerful tool for multi-elemental analysis owing to its minimal sample preparation, real-time measurement capability, and ability to simultaneously detect both light and heavy elements. When a high-energy laser pulse interacts with a material surface, it generates a micro-plasma that emits characteristic spectral lines corresponding to the elements present. However, in metals exhibiting strong matrix emission, impurity lines can be masked or overlapped by dominant transitions from the base metal.

To overcome this challenge, reference spectrum subtraction can be applied. By subtracting the emission spectrum of a pure metal from that of the corresponding sample, matrix-related lines are effectively removed, allowing impurity lines to be isolated with improved clarity and sensitivity. This approach significantly improves the detection of trace contaminants and improves the accuracy of quantitative analysis.

In this study, LIBS combined with reference spectrum subtraction was employed to analyze impurities in five metal samples: gold (Au), aluminum (Al), cobalt (Co), iron (Fe), and lead (Pb). The objective was to identify impurity species, quantify their concentrations using calibration curves, and compare impurity profiles across the different metals. The results provide insight into alloying practices, environmental exposure, and contamination pathways, while demonstrating the effectiveness of LIBS as a rapid and reliable technique for impurity screening.

2.Materials and Methods

Five metallic samples (gold, aluminum, cobalt, iron, and lead) were analyzed. Each sample, with a mass of 5 g, was cleaned with ethanol to remove surface dust and contaminants prior to LIBS measurement. No additional chemical preparation or digestion was required, thereby, preserving the non-destructive nature of the technique.

International Journal of Engineering and Information Systems (IJEAIS)
ISSN: 2643-640X
Vol. 10 Issue 3 March - 2026, Pages: 15-20

LIBS Instrumentation system **is** depicted schematically in Fig. 1. A pulsed laser source (400 nm -100mJ) was used to generate plasma on the surface of each metal sample. The emitted plasma radiation was collected by an optical fiber and directed into a spectrometer covering the wavelength range relevant to the detected impurity lines (approximately 550–800 nm, based on the impurity wavelengths in the table 1). The spectrometer (USB 2000+ has four spectrometer modules that give high resolution (FWHM 0.1 nm) and a gated CCD detector with 14,336 pixels for simultaneous spectra recording in the 400 nm to 1150 nm wavelength range) resolution was sufficient to resolve closely spaced emission lines.

Reference Spectrum Subtraction; to isolate impurity emission lines, the reference spectrum of each pure metal was recorded under identical experimental conditions. This reference spectrum was then subtracted from the corresponding sample spectrum. The subtraction process effectively eliminated matrix-related lines and enhanced the visibility of impurity transitions. The resulting spectra for all samples, as shown in Fig. 2, contained only non-matrix emission lines. The concentration of the identified elements was calculated using the calibration curve method using the total intensity of the selected spectral lines. Impurity lines were identified using their wavelengths, upper and lower energy levels(E_f, E_i), transition probabilities (A_k), and degeneracy factors (g), as listed in Table 1. Calibration curves were constructed for each detected impurity element in Fig. 3. Line intensities were plotted against known standard concentrations to derive linear regression equations. These equations were then used to convert the measured intensities into concentrations expressed in parts per million (ppm).

All spectra were processed using standard LIBS analysis procedures, including background correction, peak fitting, and normalization. The consistency of repeated lines was used to validate the reliability of the quantification.

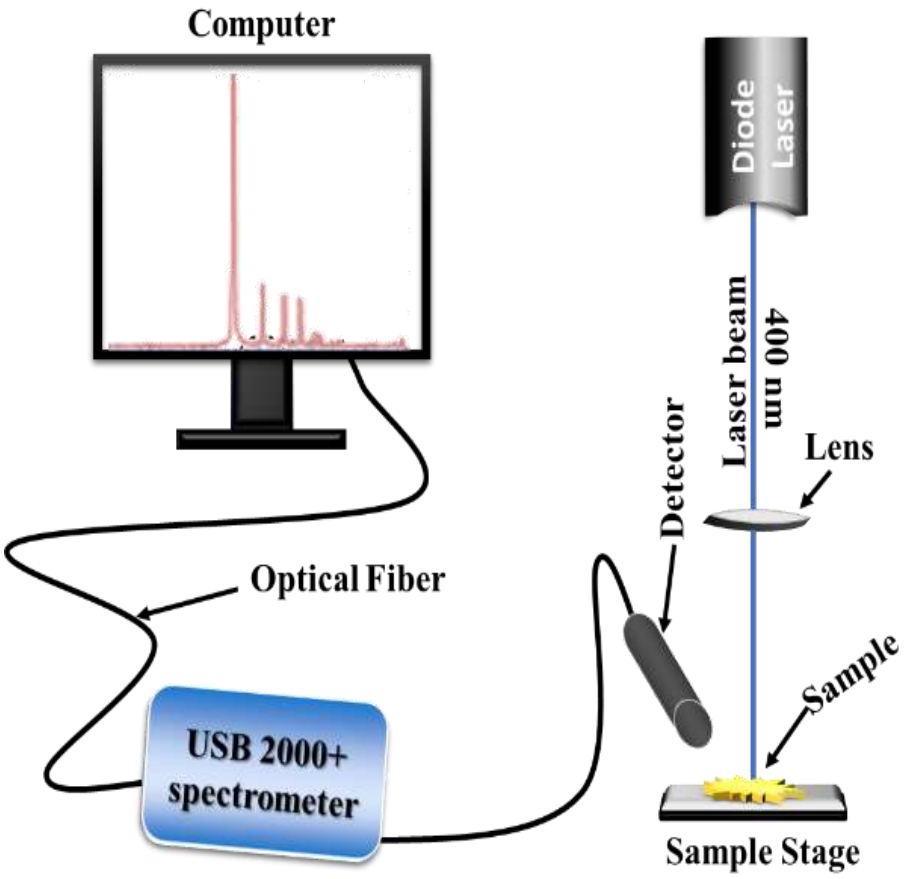

Figure 1: shows the experimental setup for LIBS evaluation of samples.

3. Results

Laser-Induced Breakdown Spectroscopy (LIBS) proved effective in detecting trace-level impurities in all five metal samples (Au, Al, Cu, Fe, and Pb). Because the reference spectrum of each pure metal was subtracted from the measured spectrum, the resulting emission lines correspond exclusively to impurity species. This subtraction approach significantly improved the signal-to-background ratio and enabled the detection of elements at concentrations down to the sub-ppm level. The impurity concentrations were calculated using calibration curves Fig. 3, and the results are summarized in Table 1. Each element provides the transition parameters and the derived concentration (C) in ppm.

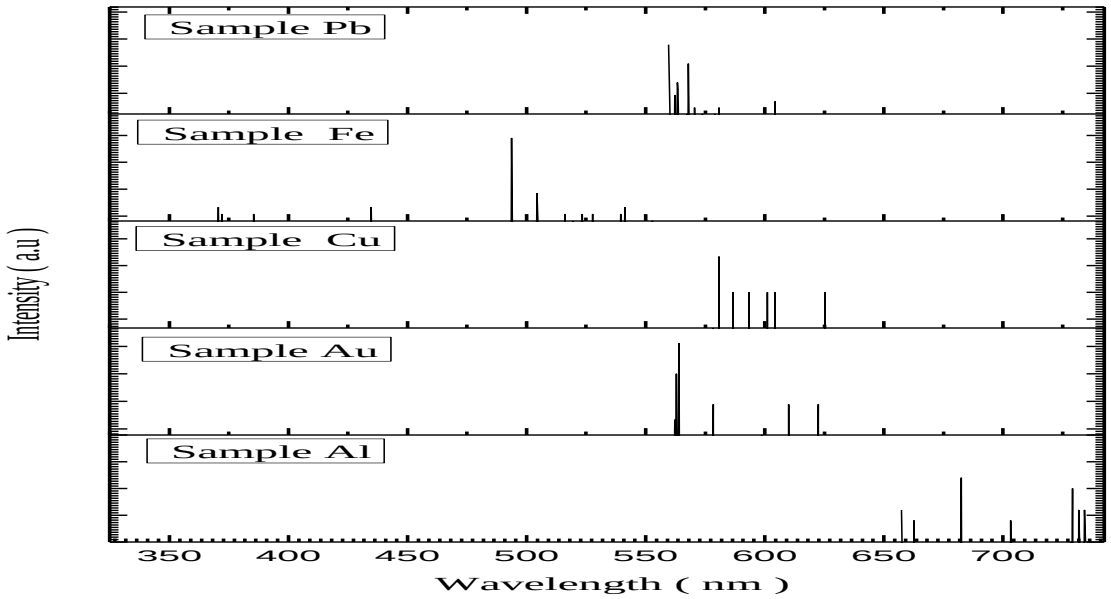

Figure 2: LIBS spectrum of (Gold, aluminum, cobalt, iron, and lead) samples irradiated by 400 mJ.

International Journal of Engineering and Information Systems (IJEAIS)
ISSN: 2643-640X
Vol. 10 Issue 3 March - 2026, Pages: 15-20

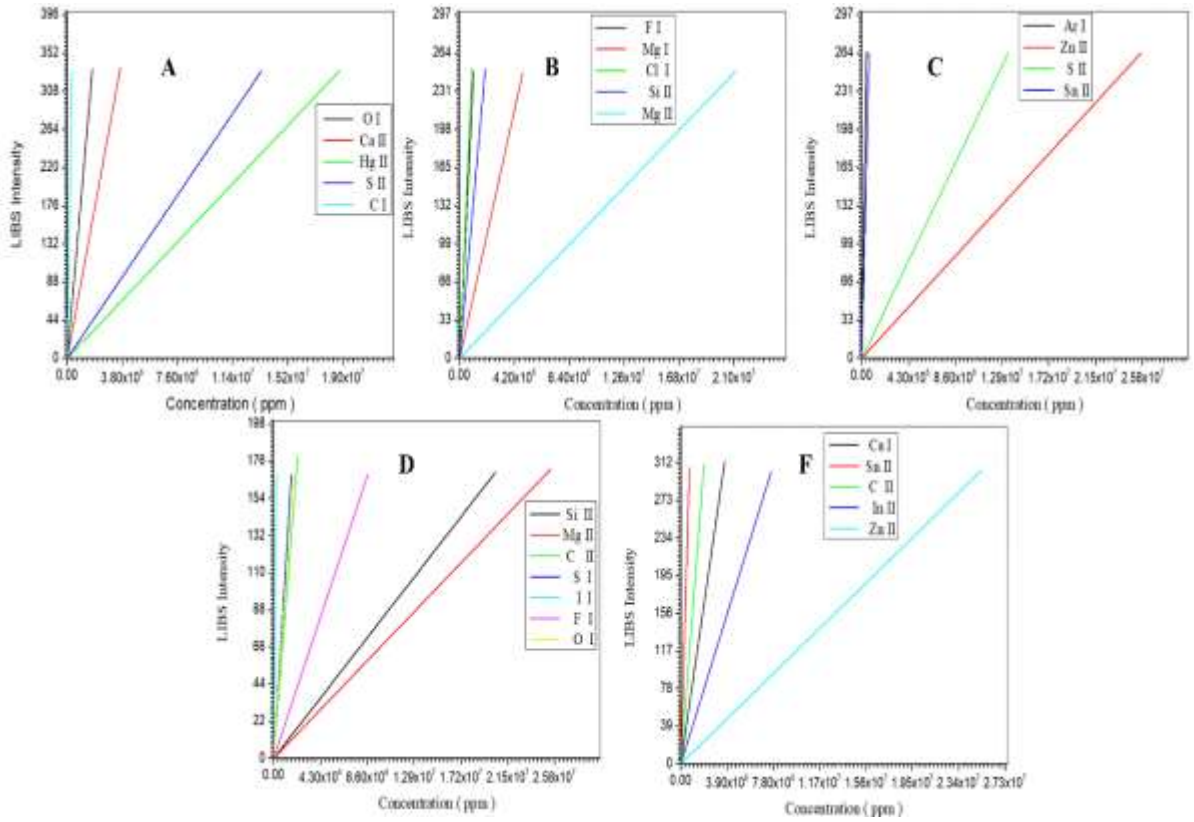

Figure 3: Calibration carves of elements present within all samples (A: Gold sample, B: Aluminum sample, C: Cobalt sample, D: Iron sample and F: Lead sample).

Table 1**:** The elements extracted from all samples (Gold, aluminum, cobalt, iron, and lead) LIBS spectrum

Sample	Element	E_f	E_i	A_k $\times 10^8$	Intensity	λ (nm)	g	N	C (ppm)
Gold sample	O I	76794.978	226.977	0.623	333	718.503	2	8	5.208
	Ca II	25191.51	0.00	1.32	335	720.219	2	20	1.0942
	Hg II	111971.464	95714.406	3.44	331	734.651	4	80	5.6586
	S II	128599.16	110268.60	0.85	331	762.974	12	16	4.0389
	Cl I	85735.091	72827.038	0.063	331	774.447	4	17	0.983
Aluminum sample	F I	119081.814	105056.283	0.38	248	712.789	2	9	2.326
	Mg I	41197.403	21911.178	0.575	246	716.554	6	12	5.109
	Cl I	85735.091	72488.568	0.12	251	754.707	6	17	2.631
	Si II	81191.34	65500.47	0.77	250	784.880	2	14	1.274
	Mg II	93799.63	71491.06	2.08	248	787.705	8	12	1.176
	Mg II	93799.63	71491.06	2.08	247	789.932	8	12	1.172
Cobalt sample	Ar I	107289.7054	93143.7653	0.0395	265	735.329	8	18	0.0616
	Zn II	117263.558	96960.588	1.6	264	747.878	12	30	0.1028
	S II	128599.16	110268.60	0.85	264	757.891	12	16	0.1961
	Sn II	39257.053	17162.499	0.26	264	774.143	2	50	0.0393
Iron sample	Si II	40991.888	6298.847	1.89	169	557.667	6	14	8.3109
	Si II	40991.888	6298.847	1.89	168	570.137	6	14	8.3111
	Si II	40991.888	6298.847	1.89	169	597.892	6	14	8.3113
	Mg II	93799.63	71491.06	2.08	171	654.597	8	12	6.7269
	C II	131735.52	116537.65	0.363	179	657.805	4	6	0.8109
	S I	55330.811	573.640	0.549	168	675.716	2	16	0.01034
	I I	75621.41	56092.88	0.030	168	681.257	6	53	0.0636

	F I	116987.391	102405.714	0.494	168	685.603	12	9	0.1943
	O I	76794.978	226.977	0.623	168	700.223	2	8	0.9441
Lead sample	Ca I	25191.51	0.00	1.32	313	714.815	2	20	0.8475
	Sn I	39257.053	17162.499	0.26	307	719.078	2	50	0.0425
	C II	145549.27	131724.37	0.352	310	723.132	4	6	0.01592
	In II	107841.54	93923.40	1.4	303	735.060	4	49	0.3977
	Zn II	117263.558	96960.588	1.6	304	758.846	12	30	0.1202

4. Discussion

The LIBS spectra obtained from the five metal samples (gold, aluminum, cobalt, iron, and lead) irradiated at 400 mJ reveal clear elemental fingerprints and impurity distributions across all materials. The spectral lines listed in the document (e.g., "Fig. 2, LIBS spectra of (Gold, aluminum, cobalt, iron, and lead) samples irradiated by 400 mJ" and "Table 1, the elements extracted from all samples") show that each sample contains both expected matrix-related emissions and trace-level contaminants.

Elemental signatures and impurity trends:

- **Gold sample:** The spectrum shows strong lines of O I, Ca II, Hg II, S II, and Cl I. The highest concentration is Hg II (5.6586 ppm), followed by O I (5.208 ppm) and S II (4.0389 ppm). The presence of oxygen and sulfur suggests surface oxidation or environmental contamination, whereas mercury may originate from refining processes. The document confirms these lines, e.g., "Hg II… C (ppm) = 5.6586".

- **Aluminum sample:** The aluminum sample exhibits emission lines corresponding to Mg I, Mg II, F I, Cl I, and Si II. Magnesium shows the highest concentration (5.109 ppm), indicating alloying or residual impurities from production process. Fluorine and chlorine (2.326 and 2.631 ppm) may be linked to chemical etching or environmental exposure. These results are clearly presented in Table 1, e.g., "Mg I… C (ppm) = 5.109".

- **Cobalt sample:** The detected impurities (Ar I, Zn II, S II, Sn II) appear at very low concentrations (<0.2 ppm), indicating high sample purity. Among these, zinc and sulfur are the most notable; however, their concentrations remain minimal. The document states "Zn II… C (ppm) = 0.1028".

- **Iron sample:** Iron shows the richest impurity spectrum, dominated by Si II, with concentrations of approximately 8.31 ppm across three wavelengths. Magnesium (6.7269 ppm) is also present at a significant level. These impurities are typical of steel alloys, where silicon and magnesium are common additives or residuals. The data in Table 1 confirm this, with "Si II… C (ppm) = 8.3109–8.3113".

- **Lead sample:** The lead sample contains Ca I, Sn I, C II, In II, and Zn II. Calcium (0.8475 ppm) and indium (0.3977 ppm) are the most prominent impurities. These may originate from ore processing or alloying. The document lists "Ca I… C (ppm) = 0.8475".

5. Conclusion

The LIBS analysis successfully identified and quantified elemental impurities in gold, aluminum, cobalt, iron, and lead samples using 400 mJ laser irradiation. The spectra presented in this study, along with the quantitative results in Table 1, demonstrate that LIBS provides rapid, sensitive, and multi-element detection across all samples.

- Each sample exhibits a distinct impurity profile, with iron showing the highest impurity levels (notably Si II), while cobalt shows the lowest.

- The presence of oxygen, sulfur, chlorine, and fluorine in several samples indicates environmental exposure or processing-related contamination.

- Calibration curves enabled accurate ppm-level quantification, confirming LIBS as a reliable tool for trace elemental analysis.

- The method effectively differentiates between high-purity and alloyed/contaminated samples, making it suitable for applications in quality control, metallurgy, and material certification.

6. References

[1] Davari, S. A., et al. (2021). Calibration-Free Quantitative Analysis of Lithium-Ion Battery Electrode Materials Using Laser-Induced Breakdown Spectroscopy (LIBS).ACS Applied Energy Materials, 4(7), 7259–7267. https://doi.org/10.1021/acsaem.1c01386
.

[2] Zhang, et al. (2023). Atomic Spectrometry Update: Review of Advances in the Analysis of Metals, Chemicals and Materials Including LIBS. Journal of Analytical Atomic Spectrometry. https://doi.org/10.1039/D3JA90038J.

[3]A Review of Calibration-Free Laser-Induced Breakdown Spectroscopy. (2022). TrAC Trends in Analytical Chemistry, 152, 116618. https://doi.org/10.1016/j.trac.2022.116618.

[4] Nouman Khan, M., et al. (2023). Evaluation of Medicinal Plants Using LIBS Combined With Chemometric Techniques. Lasers in Medical Science, 38(1), 149–?. https://doi.org/10.1007/s10103-023-03805-2.

[5] Rezaei, F., et al. (2025). A Comprehensive Review of the Fundamentals, Progress, and Applications of the LIBS Method in Analysis. Photonics, 12(11), 1061. https://doi.org/10.3390/photonics12111061.

[6]Review of Element Analysis of Industrial Materials by In-Line LIBS. (2024). Applied Sciences, 11(19), 9274. https://doi.org/10.3390/app15158640.

[7] Nurul Absar, Jainal Abedin, Md. Mashiur Rahman, Moazzem Hossain Miah, Naziba Siddique,Masud Kamal, Mantazul Islam Chowdhury, Abdelmoneim Adam Mohamed Sulieman , Mohammad Rashed Iqbal Faruque , Mayeen Uddin Khandaker, David Andrew Bradley and Abdullah Alsubaie, Radionuclides Transfer from Soil to Tea Leaves and Estimation of Committed Effective Dose to the Bangladesh Populace, Life,MDPI 2021, 11,282. https://doi.org/10.3390/life11040282.

[8] Vinicius C. Costa, Diego V. Babos,b Jeyne P. Castro, Daniel F. Andrade, Raimundo R. Gamela,b Raquel C. Machado, Marco A. Sperança, Alisson S. Araújo, José A. Garciab and Edenir R. Pereira-Filho, Calibration Strategies Applied to Laser-Induced Breakdown Spectroscopy: A Critical Review of Advances and Challenges, J. Braz. Chem. Soc., Vol. 31, No. 12, 2439-2451, 2020, https://dx.doi.org/10.21577/0103-5053.20200175.

[9] Eleonora D'Andrea, Stefano Pagnotta, Emanuela Grifoni, Stefano Legnaioli, Giulia Lorenzetti, Vincenzo Palleschi, Beatrice Lazzerini, A Hybrid Calibration-Free/Artificial Neural Networks Approach to the Quantitative Analysis of LIBS Spectra, Applied Physics B, Springer, laser and optics, volume 118, pages353-360,01 January 2015, DOI:10.1007/s00340-014-5990-z.

[10] Ashwin P. Rao, Matthew T. Cook, Howard L. Hall, and Michael B. Shattan, Quantitative Analysis of Cerium-Gallium Alloys Using a Hand-Held Laser Induced Breakdown Spectroscopy Device, Atoms 2019, 7, 84; doi:10.3390/atoms7030084,

[11] Nuclear Safety Review 2023, IAEA/NSR/2023, Printed in the IAEA in Austria August 2023.

[12] National stockpiles for radiological and nuclear emergencies: policy advice, ISBN 978-92-4-006787-5, World Health Organization 2023.